Particle & Particle Systems Characterization
www.particle-journal.com

Determination of Particle Size, Core and Shell Size Distributions of Core–Shell Particles by Analytical Ultracentrifugation

*Thomas Schmidt, Jürgen Linders, Christian Mayer, and Helmut Cölfen**

In core–shell nanoparticle analysis, the determination of size distributions of the different particle parts is often complicated, especially in liquid media. Density matching is introduced as a method for analyzing core–shell nanoparticles using Analytical Ultracentrifugation (AUC), making it possible to obtain the core size distribution in liquid dispersions. For this approach, the density of the dispersion is adjusted to the density of the shell. Oil filled nanocapsules are utilized with component densities of around 1 g mL^{-1} to demonstrate this technique. The shell size distribution is calculated supposing the particle size distribution as a convolution of the shell- and core size distributions. Finally, the distributions of core size, shell thickness, particle size, and particle density and thus particle composition are obtained. To clarify the effect of swelling, AUC measurements are combined with further size characterization methods like Particle Tracking Microscopy and Dynamic Light Scattering.

1. Introduction

Core–shell particles are a widely used class of nanoparticles. One example is the application as impact modifier for plastics.[1] Another is the use of bimetallic core–shell particles with variable optical properties usable for example as chemical sensors.[2] In medical studies, iron oxide nanoparticles coated with mitroxantrone can be used to bring the substance into a tumor, or in case of coating with special antibodies to better localize a tumor via magnetic resonance tomography and to destroy it via hyperthermia by using oscillating magnetic fields.[3] In the field of catalysis, titanium dioxide nanoparticles coated with gold are used for special redox reactions, which can be tuned by a laser pulse.[4] But in a more general sense, every nanoparticle stabilized by (macro) molecules is a core–shell particle. A special case of core–shell particles are nanocapsules. These are polymeric capsules with a fluid content and a radius between 50 and 500 nm. They can be used in medical applications, for example as carrier for anti-tumor compounds or for peptides and proteins such as insulin to make them orally ingestible.[5,6]

For the different applications it is important to know the size distribution of the core and shell. But the size determination of the different parts of core–shell particles is often difficult. There are a few methods to determine the mean sizes of cores and shells including small angle neutron scattering with contrast matching, UV–vis techniques or thermogravimetric analysis (TGA).[7] However, they do not yield whole size distributions. Transmission Electron Microscopy (TEM) is one method which is, in principle, able to yield both, the size distributions of the core and of the shell. But the particles are observed in a vacuum and not in solution, and organic matter suffers from poor electron contrast. Also in terms of statistics, the results are not immaculate because only a fraction of the particles can be imaged and counted.

These problems can be circumvented by using Analytical Ultracentrifugation (AUC). It was invented by Theodor Svedberg in the 1920s for analyzing particle dispersions and macromolecules.[8,9] In the present work, density matching is introduced as a new approach for analyzing core–shell nanoparticles. Density matching has already been successfully used to eliminate the effect of detergents on membrane proteins in ultracentrifugal fields by using H_2O/D_2O mixtures or further substances to match the density of the detergent typically in sedimentation equilibrium runs.[10,11] As a result, the density matched compound becomes "invisible" in the AUC since it will not respond to the centrifugal force. This prompted us to use density matching for core–shell nanoparticle analysis using AUC. For this method the density of the dispersion medium is adjusted to the density of one of the particle's compounds. Therefore, this compound is density matched and will not influence the separation of the particle in the centrifugal

T. Schmidt, H. Cölfen
Physical Chemistry University of Konstanz
Universitätsstr. 10, D-78457 Konstanz, Germany
E-mail: Helmut.Coelfen@uni-konstanz.de
T. Schmidt
Institute of Physical Chemistry
RWTH Aachen University
Landoltweg 2, 52074 Aachen, Germany
J. Linders, C. Mayer
Physical Chemistry and Center for Nanointegration Duisburg-Essen (CeNIDE)
University Duisburg-Essen
Universitätsstr. 5, D-45141 Essen, Germany
The ORCID identification number(s) for the author(s) of this article can be found under https://doi.org/10.1002/ppsc.202100079.

DOI: 10.1002/ppsc.202100079

field, yielding the sedimentation coefficient distribution of the unmatched compound. That way, size distributions of core and shell or the amounts of different polymers in hybrid nanoparticles can be obtained. Yielding the size, particle density or further core shell properties via AUC generally need multidimensional analysis or simulations.[12–15] Another advantage of this method is that no "core only" particles without ligands are required as a reference. Furthermore, swelling of particle shells may be evaluated by combining the AUC results with another particle sizing method.

2. Experimental Section

The nanocapsules were prepared by the method of Al Khouri Fallouh and coworkers.[16] The organic phase consisting of absolute ethanol (50 mL), Miglyol 812 (3.604 g) and *n*-Butyl-2-cyanoacrylate (0.541 g) was added in drops during stirring into a 5 percent solution of Pluronic F-68—a polyoxyethylene-polyoxypropylene block copolymer (200 mL). The dispersion obtained was stirred for 30 min and extracted three times with cyclohexane (30 mL). To remove excess surfactant, the dispersion was dialyzed against distilled water in a dialysis tube with a molecular weight cut-off value of 100 kDa for one week. The water was changed three times.

For the AUC measurement of the pure capsules, the sample was diluted with water and measured at 20 and 25 °C. For the measurements at 20 °C the dilution was 1:3 (sample to water), and 1:1 for the measurements at 25 °C. Different mixtures with different densities were prepared to investigate the swelling of the shells. The composition of the water/ethanol mixtures is summarized in Table S37 (Supporting Information). For the measurement in the acetone-water mixture 300 µL of the sample dispersion, 251 µL acetone and 49.2 µL water were mixed. The isopropanol-water mixture consisted of 300 µL sample dispersion, 212 µL isopropanol and 85.2 µL water. The composition of the mixtures is based on the literature to result in a density of 0.95 g mL^{-1}, which was controlled by using a density meter.[17,18]

For densities larger than 1 g mL^{-1}, sodium chloride mixtures were prepared. The composition is summarized in Table S38 (Supporting Information).

In all cases, the AUC reference sector mixtures were similarly with the difference that the volume of the sample was replaced by water.

The AUC measurements were performed in 20 mm double sector cells for the sedimentation velocity runs. The speeds for the different mixtures are listed in **Table 1**. To analyze the data, the program SEDFIT was used.[19,20]

2.1. Substances Used and Sources

For all experiments Milli-Q water (18.2 MΩ cm) was used except for dialysis where normal distilled water was used (internal device). Glucose was purchased from Riedel de Haën, sucrose and sodium chloride from Fisher Scientific. Glycerin, ethanol (absolute), isopropanol (p. a.) and acetone (p. a.) came from VWR. Caesium chloride was purchased from Merck, the surfactant Pluronic F-68 (Poly(ethylene oxide)-poly(propylene oxide) block copolymer) from BASF and *n*-Butyl-2-cyanoacrylate from 3M. The oil Miglyol 812 was obtained from Caesar & Lorentz GmbH.

Table 1. Overview of the conditions at which the samples were measured.

ρ (medium) [g mL^{-1}]	Speed [rpm]	Temperature [°C]
0.93	3500	25
0.95 (ethanol-water mixture)	6000	25
0.95 (acetone-water mixture)	3000	20
0.95 (isopropanol-water mixture)	3000	20
0.97	3500	25
0.98	3500	25
1.0	5000	25
1.0	5000	20
1.01	3500	20
1.02	3000	20
1.03	3500	20
1.04	3500	20
1.12	2500	20
1.13	2500	20
1.14	1500	20
1.15	1500	20

2.2. Instruments

AUC Beckman Instruments XL-A/I, detection via interference (660nm Laser Rayleigh-interferometer)

Dynamic Light Scattering **(DLS)** (own construction), laser: 633 nm power < 35 mW, single-photon-detector: PMT-120-OP/B, digital correlator: Flex 02–08D/C

Darkfield microscope (Orthoplan, Leitz), with CCD-Camera (FireWire-Cam-011H, Phytec) with self-written software

Density meter Anton Paar DMA 5000 M.

3. Results and Discussion

The sedimentation coefficient *s* is the key value obtained by AUC. It is defined as the ratio of the drift speed and the acceleration in the ultracentrifugal field and holds a unit of S (Svedberg, 1 S = 10^{-13} s). In the ultracentrifugal field the fractionated particles are recorded resolved in radial position and in time, obtaining sedimentation curves, which can be fitted with different models to get the respective *s* values or distributions.[9] We applied the sedimentation coefficient distribution *ls-g*(s)*, obtained from a least squares fit to the original sedimentation curves.[21]

To determine the hydrodynamic diameter d_h of a particle via AUC Equation (1) can be used assuming it to be a hard sphere[9]

$$d_h = \sqrt{\frac{18\eta s}{(\rho_p - \rho)}} \quad (1)$$

Therefore, the density of the particle ρ_p, the viscosity of the dispersion solvent η and the density of the dispersion solvent ρ have to be known or determined.

If the density of a particle is not known, it can be calculated with the knowledge of an independently determined d_h by converting Equation (1) into Equation (2)

$$\rho_p = \frac{18\eta s}{d_h^2} + \rho \tag{2}$$

Furthermore, characteristic values like density and size of the particle parts can be obtained and therefore knowledge about the composition of the nanocapsules is obtained.

To calculate the density of the shell, its mass has to be divided by its volume. The shell's mass is obtained by subtracting the mass of the core from the mass of the particle, which leads to Equation (3)

$$\rho_s = \frac{\rho_p V_p - \rho_c V_c}{V_p - V_c} \tag{3}$$

with c = core, p = particle, and s = shell, assuming that the density of the core is not influenced by the solution so that no swelling occurs. Because the core is protected by the surrounding shell, this assumption ought to be true. Furthermore, in our case, it is an oil which should not swell in water. The density of the shell is, however, affected by the surrounding solution and we expect it to swell.

If all densities of the compounds are known or obtained, the volume of the core can be calculated in a next step. For that, first the core mass fraction w_c has to be calculated via Equation (4).[22] This is the fraction of the core mass contributing to the particle mass

$$w_c = \frac{(1/\rho_p - 1/\rho_s)}{(1/\rho_c - 1/\rho_s)} \tag{4}$$

Thereby the core volume fraction φ_c can be calculated via Equation (5). This is the fraction of the volume occupied by core in the core–shell nanoparticles

$$\varphi_c = \frac{w_c \cdot \rho_p}{\rho_c} \tag{5}$$

If the radius of the spherical particle is known, the volume of the particle can be calculated and with the core volume fraction the size of the core can be calculated.

With our approach of density matching, we are also able to obtain size distributions of the different particle parts and not just single average values, as explained in detail below.

In this study, we investigated Pluronic-stabilized poly(*n*-butyl-2-cyanoacrylate) nanocapsules filled with Miglyol 812 oil. First, the size of the nanocapsules was measured in different ways, because the particle size is essential in this study. One method was Particle Tracking Microscopy (PTM), which yielded a number weighted hydrodynamic diameter of 327 nm ± 3 nm (**Figure 1**a) as the maximum of the distribution. Another method was Dynamic Light Scattering (DLS) which gave a mean intensity weighted value of 324 nm ± 144 nm (295 nm as the maximum of the distribution; Figure 1a). To determine the size distribution via AUC, the average density of the particles was determined by combining the PTM with the AUC measurement using Equation (2) (with the maximum values of the *s*- and PTM distributions). A value of 1.006 g mL^{-1} for particles in water at 25 °C was obtained. A second measurement at 20 °C resulted in 1.007 g mL^{-1}. The viscosities of the solvent at the different temperatures were taken from literature.[23]

To verify our results, a comparison between the measured data and the $s_{20,w}$ distribution is applied. It gives the density and viscosity corrected *s* value with respect to a standard

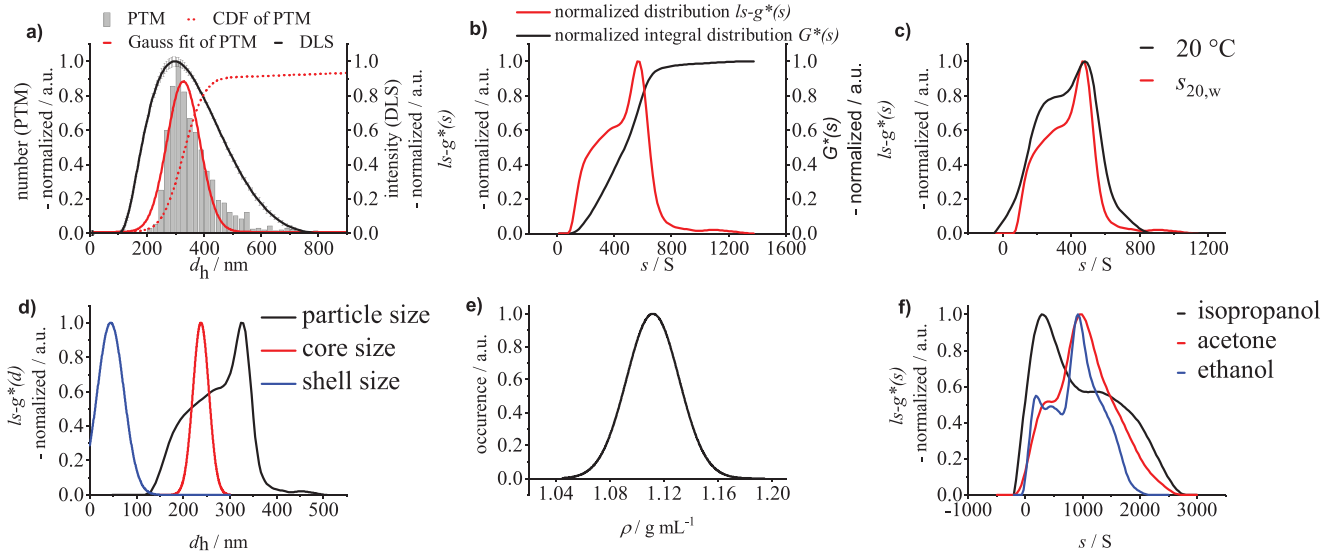

Figure 1. a) Particle Tracking Microscopy- and DLS-measurement of the nanocapsules in pure water measured at 25 °C, b) AUC-measurement of the nanocapsules in pure water measured at 25 °C and 5000 rpm (*s* distribution), c) AUC-measurement of the nanocapsules in pure water measured at 20 °C (*s* distribution) and 5000 rpm and $s_{20,w}$ distribution (calculated from the *s* distribution measured at 25 °C), d) size distribution of core, shell and the entire nanocapsules, e) density distribution of the nanocapsules in NaCl solutions with densities between 1.12 and 1.15 g mL^{-1} (see also Figure S18 in the Supporting Information), f) AUC-measurements of the nanocapsules measured in mixtures of water with: acetone, isopropanol and ethanol at a density of 0.95 g mL^{-1} (condition for the measurement in the water/ethanol mixture: 25 °C and 6000 rpm, for the other ones: 20 °C and 3000 rpm).

measurement in water at 20 °C. The $s_{20,w}$ distribution was calculated from the *s* distribution measured in water at 25 °C using Equation (6)[24]

$$s_{20,w} = \frac{(1-\overline{\nu}\rho)_{20,w} \cdot \eta_{T,b}}{(1-\overline{\nu}\rho)_{T,b} \cdot \eta_{20,w}} \cdot s_{T,b} \quad (6)$$

Here the index *T*,b represents the condition in the second medium b with the temperature *T* and the index w the condition in water. The partial specific volume $\overline{\nu}$ is the volume that is replaced by one gram of the particle (reciprocal of its density) respectively the volume increase of the surrounding solution. The *s* distributions of the measurements at 20 and 25 °C as well as the $s_{20,w}$ distribution are presented in Figure 1b,c. As visualized in Figure 1c, the maxima of the distributions are almost at the same position, revealing that no significant friction effects occur, which would alter the results of the matching experiments described later. The reason why the *s* distribution looks bimodal could be that parts of the polymer or surfactant dissolve as has been described for microgels in the literature.[25]

Furthermore, it is possible to determine not only the density but the density distribution. For this we used the normalized integrated *s*- and integrated PTM distribution (Figure 1a,b) calculated with Equation (2) using sampling points between 0 and 1 with a step width of 0.1 and obtained density values between 1.005 and 1.007 g mL^{-1} (Figure S1, Supporting Information). Because the fluctuations are smaller than the standard deviation of the sedimentation coefficient from AUC (4.4%), we considered the value to be constant.[26] Using a density of 1.006 g mL^{-1} we calculated the size distribution visualized in Figure 1d.

Because the diameter of the nanocapsules has already obtained, the volume of the nanocapsules can be calculated as well as the volume and the diameter of the core. A diameter of 290.6 nm was obtained using Equations (4) and (5) with a density of 0.95 g mL^{-1} for the oil (Miglyol 812) and 1.142 g mL^{-1} for the shell (polybutylcyanoacrylate).[22] However, the determined core size is just a one value and not a distribution and it relies on a fixed shell density, which is not correct if the shell swells. Moreover, since the capsule membrane is formed by interfacial polymerization, the thickness of the capsule wall will necessarily depend on the local monomer concentration during the preparation. The monomer concentration on the other hand is not only time dependent, but will also vary with the given location, both dependencies being caused by local reaction and diffusion processes. In consequence, we can expect a Gaussian distribution of capsule wall thicknesses, which is not linked to capsule size.

We therefore applied the density matching of the shell to independently determine the core size distribution.Thus, a compound must be found which raises the solvent density without forming a density gradient in the centrifugal field during the experiment and without destabilizing the particles. Different agents such as glucose, sucrose, glycerin and caesium chloride were tested but they formed a gradient in the ultracentrifugal field even at low speeds. Using NaCl yielded good results. No gradient was formed and the particles remained stable even at NaCl concentrations of 20 wt% as tested by DLS (Figure S2, Supporting Information).

To match the shell of the particles, the density has to be adjusted to a region around 1.15 g mL^{-1}, the density of the shell material. To calculate the density distribution of the capsules with matched shells, different mixtures with densities in that region (between 1.12 and 1.15 g mL^{-1}) were prepared and measured in the AUC. Additionally, the normalized integrals *G*(s)* of the distributions were calculated (Figures S3–S6, Supporting Information). These *G*(s)* distributions can be regarded as cumulative distributions. To calculate the density of the capsules in the NaCl solutions we used a modified method introduced by Tziatzios and coworkers, plotting the sedimentation coefficient against the solvent density.[27] We first chose sampling points between *G*(s)* = 0 and *G*(s)* = 1 with a distance of 0.1 of the normalized integrals of the *G*(s)* distributions and obtained the respective *s*-values. Therefore, we received 11 sampling points for each of the four measured distributions. In a second step we plotted for each *G*(s)* value all 4 respective *s* values against the density where the *s* value was received from. These 11 graphs visualizing the density dependent sedimentation coefficients are depicted in (Figures S7–S17, Supporting Information). Thus, the density of the capsules is now obtained as the intercept with the x-axis for each *G*(s)* value. Since *G*(s)* can be regarded as a cumulative distribution, we could link the obtained density values to a certain occurrence and fitted the values with a normal cumulative density distribution function (Figure S18, Supporting Information). Differentiating and normalizing the resulting curve, the density distribution in NaCl at core matching conditions as visualized in Figure 1e was obtained.

Using the cumulative density distribution (Figure S18, Supporting Information) and the normalized integral *s* distribution under shell matching conditions (Figure S6, Supporting Information) obtained from the mixture with a density of 1.15 g mL^{-1}, we calculated via Equation (1) single values of the core size distribution and fitted them with a normal cumulative distribution function, connecting each density value to an *s* value of the distributions (Figure S19, Supporting Information). We calculated from this the derivative as visualized in Figure 1d. Compared with the average values calculated before, these values seem to be too low. Independently, the mass-weighted value of the s distribution under shell matching conditions (Figure S6, Supporting Information) was calculated with the program SEDFIT yielding a value of –1020.47 S and a diameter of 274.08 nm.[20] This fits to the value calculated before by only using the densities of the compounds (290.6 nm). and confirms the validity of the core size distribution.

Similarly, density matching of the core should permit calculation of size distribution of the shell. In this case not the shell thickness but the size of a spherical particle with the same volume like the shell would be obtained. To calculate the shell thickness, the core volume needs to be added. From the resulting size distribution of the whole particle and the core size distribution, the shell thickness distribution could be calculated. On the other hand, the swelling of the shell is expected to depend on the solvent, therefore this approach is less suitable.

As the particle size and the core size of the particle are known as distributions, the shell thickness distribution can

be calculated even under the conditions of shell swelling. Regarding the size distribution as convolution of the shell and core size distributions, we calculated the shell thickness using the PTM based particle size distribution and the core size distribution, assuming that both distributions can be described by normal distributions. For this we used the relation that $\mu = \mu_1 + \mu_2$ and $\sigma = \sqrt{(\sigma_1 + \sigma_2)}$. The shell thickness distribution is visualized in Figure 1d (as normalized distribution). Because of the model of capsule formation, we expected Gaussian normal distributions for the different sizes of the fragments. These arise due to the fact that the drops are statistically distributed in the dispersion where the monomer is reacting at their surface. The shell thickness is influenced by concentration fluctuations of the monomer. It is additionally influenced by the diffusion of the drops and capsules as well as of the monomer. Thus, a variety of statistical processes make a Gaussian distribution of the different fragment sizes most likely. Therefore, if we calculate back the whole particle size distribution with a Gaussian core and shell size distribution, we would get a Gaussian particle size distribution as it is indicated by the density independent PTM distribution in Figure 1a. This is the justification for a Gaussian particle size distribution even if the sedimentation coefficient distribution is bimodal since it is a folded distribution depending on particle size and density. Because in the *ls-g*(s)* method the diffusion broadening is not taken into account, the values of the main particle size seem to be lower than the ones from the core size. However, the lowest values of size distribution obtained by PTM and of the core size distribution correspond well to each other.

To demonstrate the effect of swelling of the shell in different solvents, mixtures in ethanol/water, acetone/water and isopropanol/water, all with a density of 0.95 g mL^{-1} (the density of the oil core) were prepared and measured in the AUC. The composition of the mixtures can be found in the experimental section. The resulting *s* distributions are depicted in Figure 1f. The related DLS measurements can be found in the Supporting Information (Figures S20–S22, Supporting Information) to clarify that no particle aggregation occurs. In the various mixtures different swelling of the shell occurs as indicated by the different shape of the *s* distributions.

To determine the swelling of the capsules more precisely, different AUC measurements with media in a density region between 0.93 and 1.04 g mL^{-1} were realized, by mixtures of ethanol and water for densities lower 1 g mL^{-1} and aqueous NaCl solutions for higher densities (Figures S23–S29, Supporting Information).

The maxima of the *s* distributions were plotted against the density of the medium (**Figure 2**a). A nearly straight line is obtained. For media densities larger than the particle density, the sedimentation coefficient is negative due to flotation. The mixtures with densities between 0.94 and 0.96 g mL^{-1} were left out because this is the region of the oil's density and matching effects could occur. The errors on the sedimentation coefficient were quite low in a range between 0.01 and 0.03 for the root mean square deviation of the *ls-g*(s)* method, indicating that our measurements yield relevant results.

The same samples were also investigated by Particle Tracking Microscopy and DLS to obtain size information of the particles (in terms of densities lower than 1 g mL^{-1} with PTM, for higher densities with DLS; Figures S30–S36, Supporting Information). The physical data needed, such as viscosities and refractive indices were taken from the literature.[21,28] The maxima of the size distributions plotted against the density, also yield a nearly straight line with a few outliers (Figure 2b). The swelling seems to have a linear behavior. For obtaining the error bars of the size values, we took the error on fitting the maximum of the Gaussian in case of the PTM measurements. In the case of the DLS measurements we used the 6^{th} root of the error of the intensity weighted mean. The errors of the sizes and of the sedimentation coefficient were used to calculate the errors on the further calculated values in terms of error propagation.

Combining the size and the sedimentation coefficient (maxima of the distributions) using Equation (2), the density of the particles can be calculated because this density is dependent on the density of the surrounding medium (Figure 2c). Plotting theses values, also in this case a straight line is obtained. It has to be mentioned that the increase is small compared with the size change.

From that, the density of the shell can be calculated using Equation (3) with the allready calculated core diameter of 290.6 nm and particle sizes (converted to a volume) and the density of the oil of 0.95 g mL^{-1}. Plotting the shell density against the density of the medium, one obtains the diagram illustrated in Figure 2d. Also, in this case a straight line (with a few outliers) is obtained, indicating a small increase of the shell density with the density of the surrounding medium. The errors for the values obtained at higher densities are slightly higher because of the greater errors of the DLS measurements.

Because the radii of the capsules and the core are known, the mean shell thickness is obtained (Figure 2e) by subtracting the core size from the particle size. Plotting the thickness against the density of the medium also gives a straight line. It is conceivable that there is not only a swelling effect, but also an extension of the shell by the Pluronic surfactant molecules resulting in a larger size. Namely the observed shell thickness of up to 165 nm compared to the lowest one of almost 10 nm indicates that the growth is not only resulting from the swelling of the polymer shell. Possibly ethanol molecules are additionally coordinated to the oxygen atoms of the surfactant, a polyoxamer, resulting in the extension.

To determine the volume swelling degree Q_p of a particle, the quotient of the volumes of the swollen and the unswollen particle has to be formed. Because in our case it was challenging to determine the unswollen state of the particle, the one with the smallest measured diameter (309.4 nm) was chosen. Using this, the result seen in Figure 2f was obtained.

Because the volume of the shell can be calculated by subtracting the volume of the core from the particle volume, also the degree of swelling of the shell could be calculated, as seen in Figure 2g. While Q_p was comparatively low (Q_p = 1–8), the degree of swelling increased up to Q_s = 42 for the shell (Figure 2g). This is because the shell is thin compared to the whole particle and only the shell, which is most subject to swelling, leads to higher degrees of swelling.

Furthermore, the distribution of the nanoparticle composition can be calculated from the particle density ρ_p in terms of the mass fraction *w* using the known densities of core (c) and shell

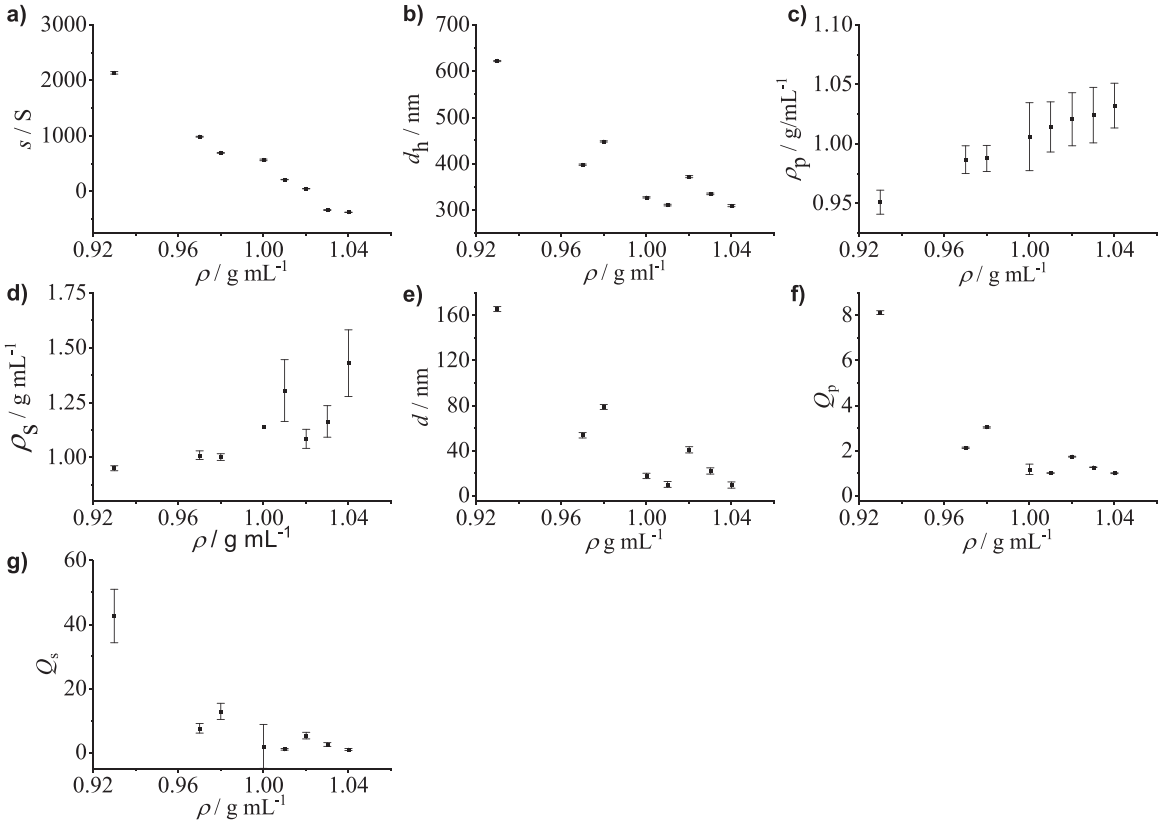

Figure 2. a) The dependence of the nanocapsule sedimentation coefficient on the density of the medium (the data points represent the maxima of the measured *s* distributions) b) size dependence of the nanocapsules on the density of the medium, c) dependence of the nanocapsule density on the density of the medium, d) dependence of the shell density on the density of the medium, e) dependence of shell thickness on the medium density, f) dependence of the degree of swelling of the nanocapsules *Q* on the medium density, g) dependence of the degree of swelling *Q* of the shell on the medium density. The error bars were calculated by error propagation of errors in size and sedimentation coefficient.

(s) in Equation (4). For this we used the density distribution of the nanocapsules in water (Figure S1, Supporting Information). As described previously, the values obtained lie between 1.005 and 1.007 g mL^{-1}. They can thus be regarded as constant, taking the precision of the method into consideration. The densities of core (0.95 g mL^{-1}) and shell (1.142 g mL^{-1}) are also regarded as constant, because the oil cannot swell in water and since the particle density is constant, the density of the shell also has to be constant. As seen from **Figure 3**a, the core and shell mass fraction give a constant value each of $w_c = 0.669$ and $w_s = 0.331$ or in terms of the core/shell volume fraction of $\varphi_c = 0.708$ and $\varphi_s = 0.292$ calculated via Equation (5). Even though our particular system gives a constant value, our method should be able to yield distributions. In this case we expect the core/shell mass and volume fractions to exhibit cumulative distribution functions, as they are calculated from the cumulative distribution functions of the different density distributions, which are in our case constant.

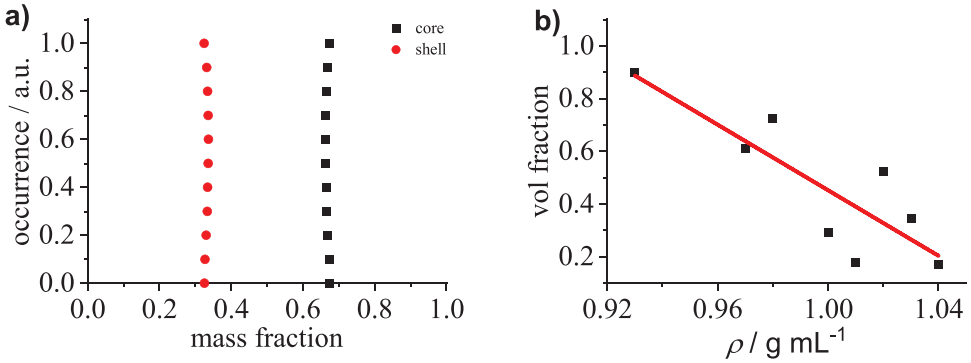

Figure 3. Composition of the nanocapsules. a) Calculated distributions of the core and shell mass fractions give a constant value for the case of the nanocapsule dispersion in water. b) dependence of core volume fraction of the nanocapsules on the surrounding medium and a linear fit to the data.

We furthermore calculated the composition of the nanocapsules for dispersions in the mixtures described of water/ethanol and water/NaCl, using additionally the Equations (2) and (3) to calculate the density of the shell under the respective conditions. As depicted in Figure 3b, the core volume fraction of the investigated nanocapsules decreases with increasing density of the surrounding medium. The values range from $\varphi_c = 0.898$ in water/ethanol (0.93 g mL^{-1}) to $\varphi_c = 0.171$ in water/NaCl (1.04 g mL^{-1}). These calculations demonstrate the large influence of swelling on the nanoparticle composition, which can vary greatly, depending on the surrounding medium.

4. Conclusion

The new AUC density matching method can yield good results for determining the core size distribution of nanocapsules. The shell thickness distribution is obtained from the core size distribution and the particle size distribution, which can be independently determined once the density distribution of the nanocapsules is known via sedimentation experiments in solutions of different densities. This yields, for the first time whole distributions of core, shell thickness, particle size, and particle density for nanocapsules. It was also possible to determine the swelling of the shell by combining an independent method for the determination of particle size distributions including PTM with AUC.

Such information is invaluable for the characterization of nanocapsules, or more general core–shell nanoparticles because it additionally yields the nanoparticle composition.

For application of this method to diverse core–shell particles, further high-density solvents, solutions, or solvent mixtures should be found to match polymers with densities higher than 1 g mL^{-1}. These materials must not form a gradient in the centrifugal field and the particles must be stable in the correspondent solutions. This does certainly limit the applicability of our method. In our case, the capsules were stable in sodium chloride solution, which is not true for all nanoparticles.[29] A further disadvantage is that it is not yet possible to match high densities (>2 g mL^{-1}) in solution without adding very dense salts in high concentrations, so that the method is not yet applicable for typical inorganic nanoparticles including the important semiconductor and metal nanoparticles.

Supporting Information

Supporting Information is available from the Wiley Online Library or from the author.

Acknowledgements

The authors thank the particle analysis center of the SFB 1214 for the possibility to perform the DLS.

Open access funding enabled and organized by Projekt DEAL.

Conflict of Interest

The authors declare no conflict of interest.

Data Availability Statement

Research data are not shared.

Keywords

analytical ultracentrifugation, core–shell particles, density matching, particle density distribution, particle size distribution

Received: April 10, 2021
Revised: June 28, 2021
Published online:

[1] J.-S. Lee, F.-C. Chang, *Polym. Eng. Sci.* **2004**, *44*, 1885.
[2] Y. Yang, J. Shi, G. Kawamura, M. Nogami, *Scr. Mater.* **2008**, *58*, 862.
[3] S. Laurent, D. Forge, M. Port, A. Roch, C. Robic, L. Vander Elst, R. N. Muller, *Chem. Rev.* **2008**, *108*, 2064.
[4] A. Dawson, P. V. Kamat, *J. Phys. Chem. B* **2001**, *105*, 960.
[5] L. Illum, P. D. Jones, R. W. Baldwin, S. S. Davis, *J. Pharmacol. Exp. Ther.* **1984**, *230*, 733.
[6] C. Damgé, C. Michel, M. Aprahamian, P. Couvreur, J. P. Devissaguet, *J. Controlled Release* **1990**, *13*, 233.
[7] R. Ghosh Chaudhuri, S. Paria, *Chem. Rev.* **2012**, *112*, 2373.
[8] T. Svedberg, J. B. Nichols, *J. Am. Chem. Soc.* **1923**, *45*, 2910.
[9] W. Mächtle, L. Börger, *Analytical Ultracentrifugation of Polymers and Nanoparticles*, Springer Berlin Heidelberg, Berlin, Heidelberg, Germany **2006**.
[10] C. Tanford, J. A. Reynolds, *Biochim. Biophys. Acta, Rev. Biomembr.* **1976**, *457*, 133.
[11] G. Mayer, B. Ludwig, H. W. Müller, J. A. van den Broek, R. H. E. Friesen, D. Schubert, in *Analytical Ultracentrifugation V* (Ed: H. Cölfen), Vol. *113*, Springer, Berlin, Heidelberg, Germany **1999**, pp. 176–181.
[12] M. J. Uttinger, S. Boldt, S. E. Wawra, T. D. Freiwald, C. Damm, J. Walter, D. Lerche, W. Peukert, *Part. Part. Syst. Charact.* **2020**, *37*, 2000108.
[13] J. Walter, G. Gorbet, T. Akdas, D. Segets, B. Demeler, W. Peukert, *Analyst* **2017**, *142*, 206.
[14] B. Demeler, T.-L. Nguyen, G. E. Gorbet, V. Schirf, E. H. Brookes, P. Mulvaney, A. a. O. El-Ballouli, J. Pan, O. M. Bakr, A. K. Demeler, B. I. Hernandez Uribe, N. Bhattarai, R. L. Whetten, *Anal. Chem.* **2014**, *86*, 7688.
[15] R. P. Carney, J. Y. Kim, H. Qian, R. Jin, H. Mehenni, F. Stellacci, O. M. Bakr, *Nat. Commun.* **2011**, *2*, 335.
[16] N. Al Khouri Fallouh, L. Roblot-Treupel, H. Fessi, J. P. Devissaguet, F. Puisieux, *Int. J. Pharm.* **1986**, *28*, 125.
[17] K. Noda, M. Ohashi, K. Ishida, *J. Chem. Eng. Data* **1982**, *27*, 326.
[18] A. Mialdun, V. Yasnou, V. Shevtsova, A. Königer, W. Köhler, D. Alonso de Mezquia, M. M. Bou-Ali, *J. Chem. Phys.* **2012**, *136*, 244512.
[19] SEDFIT version 14.81 by Schuck, Peter (NIH/NIBIB) [E], https://sedfitsedphat.nibib.nih.gov/software/default.aspx.
[20] P. Schuck, *Biophys. J.* **2000**, *78*, 1606.
[21] P. Schuck, P. Rossmanith, *Biopolymers* **2000**, *54*, 328.
[22] M. Wohlgemuth, W. Mächtle, C. Mayer, *J. Microencapsulation* **2000**, *17*, 437.
[23] I. S. Khattab, F. Bandarkar, M. A. A. Fakhree, A. Jouyban, *Korean J. Chem. Eng.* **2012**, *29*, 812.
[24] S. Uchiyama, F. Arisaka, in *Analytical Ultracentrifugation: Instrumentation, Software, and Applications* (Eds: S. Uchiyama, F. Arisaka, W. F. Stafford, T. Laue), Springer Japan, Tokyo, Japan **2016**, pp. 9–10.

[25] H.-G. Müller, A. Schmidt, D. Kranz, in *Progress in Analytical Ultracentrifugation* (Ed: W. Borchard), Steinkopff, Darmstadt, Germany **1991**, pp. 70–75.

[26] H. Zhao, R. Ghirlando, C. Alfonso, F. Arisaka, I. Attali, D. L. Bain, M. M. Bakhtina, D. F. Becker, G. J. Bedwell, A. Bekdemir, T. M. D. Besong, C. Birck, C. A. Brautigam, W. Brennerman, O. Byron, A. Bzowska, J. B. Chaires, C. T. Chaton, H. Cölfen, K. D. Connaghan, K. A. Crowley, U. Curth, T. Daviter, W. L. Dean, A. I. Díez, C. Ebel, D. M. Eckert, L. E. Eisele, E. Eisenstein, P. England, C. Escalante, J. A. Fagan, R. Fairman, R. M. Finn, W. Fischle, J. G. de la Torre, J. Gor, H. Gustafsson, D. Hall, S. E. Harding, J. G. H. Cifre, A. B. Herr, E. E. Howell, R. S. Isaac, S.-C. Jao, D. Jose, S.-J. Kim, B. Kokona, J. A. Kornblatt, D. Kosek, E. Krayukhina, D. Krzizike, E. A. Kusznir, H. Kwon, A. Larson, T. M. Laue, A. Le Roy, A. P. Leech, H. Lilie, K. Luger, J. R. Luque-Ortega, J. Ma, C. A. May, E. L. Maynard, A. Modrak-Wojcik, Y.-F. Mok, N. Mücke, L. Nagel-Steger, G. J. Narlikar, M. Noda, A. Nourse, T. Obsil, C. K. Park, J.-K. Park, P. D. Pawelek, E. E. Perdue, S. J. Perkins, M. A. Perugini, C. L. Peterson, M. G. Peverelli, G. Piszczek, G. Prag, P. E. Prevelige, B. D. E. Raynal, L. Rezabkova, K. Richter, A. E. Ringel, R. Rosenberg, A. J. Rowe, A. C. Rufer, D. J. Scott, J. G. Seravalli, A. S. Solovyova, R. Song, D. Staunton, C. Stoddard, K. Stott, H. M. Strauss, W. W. Streicher, J. P. Sumida, S. G. Swygert, R. H. Szczepanowski, I. Tessmer, R. T. I. V. Toth, A. Tripathy, S. Uchiyama, S. F. W. Uebel, S. Unzai, A. V. Gruber, P. H. von Hippel, C. Wandrey, S.-H. Wang, S. E. Weitzel, B. Wielgus-Kutrowska, C. Wolberger, M. Wolff, E. Wright, Y.-S. Wu, J. M. Wubben, P. Schuck, *PLoS One* **2015**, *10*, 0126420.

[27] C. Tziatzios, H. Durchschlag, B. Sell, J. A. van den Broek, W. Mächtle, W. Haase, J. M. Lehn, C. H. Weidl, C. Eschbaumer, D. Schubert, U. S. Schubert, in *Analytical Ultracentrifugation V* (Ed: H. Cölfen), Springer Berlin Heidelberg, Berlin, Heidelberg, Germany **1999**, pp. 114–120.

[28] R. C. Weast, *CRC Handbook of Chemistry and Physics*, 58th ed. (Ed: R. C. Weast), CRC Press, Boca Raton, USA **1977**.

[29] J. N. Israelachvili, *Intermolecular and Surface Forces*, 3 ed., Academic Press, San Diego, CA **2011**.